

# Impedance And Polarization Study of Mild Steel Corrosion In 1 M HNO<sub>3</sub> Acid Solution Using White Snakeroot (*Ageratina Altissima*) Extracts As Green Inhibitors

Ugi, B. U

Obeten, M. E.

Department of Chemical Sciences, Cross River University of Technology,  
Calabar – Nigeria

**Abstract:** *The corrosion inhibition performance of ethanol extracts from crude alkaloid, ethanol and saponin extracts of *Ageratinaaltissima*, (CAEAA), (CEEAA) and (CSEAA), respectively on the corrosion of mild steel in 1 M HNO<sub>3</sub> solutions at 30, 40, and 60°C was investigated using the conventional gravimetric, gasometric techniques, electrochemical impedance spectroscopy, potentiodynamic polarization and scanning electron microscope methods. The results suggested that both plant extracts were appreciably good inhibitors of mild steel. Inhibition efficiency was found to increase with increase in concentration and decrease with increasing temperature. The Langmuir adsorption isotherm provided acceptable linear fits based on the near unity values of the correlation coefficient values. Negative values of  $\Delta G_{ads}$  indicated spontaneity and stability of the adsorption layer. Physical adsorption mechanism is proposed for the adsorption of the components of the extracts on the metal surface.*

**Keywords:** *Ageratinaaltissima, SEM, EIS, adsorption, thermodynamics, hydrogen evolution, enthalpy*

## I. INTRODUCTION

Acid pickling, acid cleaning, acid descaling etc are common industrial activities which involves the use of routine acid solutions. Corrosion of metallic structures and subsequent deterioration of metal and its intrinsic properties are common consequences arising from aggressive acidic environment (Sudersham et al., 2016; Louis et al., 2017; Ugi et al., 2016a). As a result of efficiency, inherent stability, relatively high inhibition efficiency at considerably low concentrations and cost effectiveness, the use of organic inhibitors has been identified as the best methods of mitigating metal corrosion. Use of inhibitors is one of the most practical methods for protection against corrosion especially in acid solutions to prevent unexpected metal dissolution and acid consumption

Organic inhibitors that contain N, S, and O heteroatoms as well as pi-electron systems have been documented to exhibit good anticorrosion properties. The inhibition potential of an organic compound depends on its ability to absorb on

metallic surface (Sudersham et al., 2016; Ugi and Magu 2017). In other words the inhibitive effect of an organic compound is usually premised on the displacement water molecules from the surface of the metal and subsequent formation of protective film of the inhibitor molecules on the metal surface according to (Sudersham et al., 2016). The use of chemical inhibitors has been limited because of the environmental threat, recently due to environmental regulations. Plant extracts including their leaves, roots, tuber, stems and bark have been widely examined.

As a contribution to the current interest on environmentally friendly corrosion inhibitors, the present study is aimed at investigating the inhibiting effects of crude alkaloid, saponin and ethanol leave extracts of *Ageratinaaltissima* on the corrosion of mild steel in HNO<sub>3</sub> solution at different temperatures. The corrosion inhibition performances of the crude extracts were investigated using gravimetric and gasometric techniques electrochemical impedance spectroscopy technique (EIS), potentiodynamic

polarization techniques (PDP), and scanning electron microscopy (SEM).

## II. EXPERIMENTATION

### A. METAL COUPONS AND AGGRESSIVE SOLUTION PREPARATION

The chemical composition of the coupon used for this experiment is of the following chemical composition (wt.%) of Mn (0.99), (0.15), P (0.022), S (0.025) and Si (0.31) and Fe (balance). The mild steel used for the electrochemical studies was cut from the mild steel sheet and soldered at one end with an insulated copper wire and embedded in a chemical epoxy resin leaving the exposed surface area of 1 cm<sup>2</sup>. Prior to each electrochemical measurement, the mild steel specimens were abraded with emery papers of various grade sizes ranging from 100, 150, 320, 400, 600, 1000 and 1500, rinsed with double distilled water, degreased with acetone and air dried at room temperature. The properly ground and polished mild steel specimens were also used for SEM studies. The black acid solution (1 M HNO<sub>3</sub>) was prepared by diluting the analytical grade nitric acid with double distilled water. Various concentrations (1, 2.0, 3.5, 7.0 and 10.0 g/L) of each of the crude alkaloid extracts (CAEAA), crude saponin extract (CSEAA) and crude ethanol extract (CEEAA) were also prepared and used as inhibitors for mild steel corrosion in 1 M HNO<sub>3</sub>.

### B. INHIBITORS PREPARATION

Leaves of *Ageratinaaltissima* were obtained from Calabar, Nigeria. The plant material was identified by a botanist at the Department of Botany, University of Calabar, Calabar, Nigeria. These were dried in a MEMMERY UNB – 500 laboratory oven at 50°C and ground into powdered form. 100 g of the powdered samples was used for the extraction which was done continually with 200 cm<sup>3</sup> of absolute ethanol in a Soxhlet extractor for 2 days. The solvents were evaporated to afford crude ethanol extract. 15 g crude ethanol extract was shared into 200 ml chloroform and 200 ml 0.5 M HCl acids through the aid of a separating funnel and allowed for 1 hour. The HCl solution in the float fraction was diluted with ammonia solution and this was taken well above pH 7. Chloroform was immediately added and the layer with the chloroform eventually taken away from the funnel and distilled off. A small quantity of moderately pure crude alkaloids was obtained. In another experiment, 5g of extract in 30 ml of 20% methanol was heated for 4 hrs. in a water bath to reduce volume of ethanol to 15 mls. 20 mls diethyl ether was added to separate organic portion from the aqueous. The organic portion was discarded. This was followed by the addition of 15ml butanol to the methanolic fraction to 30ml methanol/n-butanol fraction while both mixtures were evaporated to dryness to obtain a crystalline soapy extract which was used as the saponin extract. From the stock solution (15 g/L), plant extracts test solutions were prepared at concentration of 1.0, 2.0, 3.5, 7.0 and 10.0 g/L.

### C. GRAVIMETRIC MEASUREMENTS

The test coupons were weighed and immersed in 100 ml electrolytic solution for 1 hour in the absence and presence of various concentrations of inhibitor at studied temperatures. After immersion time the coupons of various metals were picked out, cleaned with distilled water, rinsed with ethanol and degreased with acetone and immediately air dried. The specimens were weighed using electronic balance (sensitivity up to 0.0001gm). The corrosion rate (R<sub>c</sub>) of the metal and Inhibition efficiency (%IE) of inhibitors were calculated from equation 1 and 2.

$$R_c = \frac{Wl \times 1000}{At}$$

$$IE\% = \left( \frac{R_o - R_i}{R_o} \right) \times 100$$

where R<sub>o</sub> and R<sub>i</sub> are the corrosion rates in the absence and presence of the plant extracts.

### D. GASOMETRIC MEASUREMENTS

100ml of the corrodent (1 M HNO<sub>3</sub>) was introduced into a two-necked flask and the initial volume of the air in the burette was noted. Thereafter, a mild steel coupon of dimension 2cm x 0.08cm x 4cm already weighed was dropped into the corrodent and the flask was quickly closed. The volume of the hydrogen gas evolved from the corrosion reaction was monitored by volume changes in the level of paraffin oil in the graduated burette at fixed time intervals. This volume changes in the level of paraffin oil was recorded every minute for 1 hour.

#### 2.4 Electrochemical measurements

These experiments were conducted with a three-electrode electrochemical cell assembly. Well polished mild steel coupons with an surface area of 1 cm<sup>2</sup> was employed as the working electrode (WE), platinum rod as the counter electrode (E) and saturated calomel electrode as the reference electrode (RE). The RE was coupled with a luggin capillary to ensure suitable geometry of the cell electrodes with minimum potential drop. The WE was immersed in the test solution for 1 – 2 hours to attain a steady open circuit potential (OP) before each electrochemical measurement. Impedance spectra were recorded at E<sub>corr</sub> in the frequency range 10 kHz to 1 Hz with the ac voltage amplitude of 0.005V. potentiodynamic anodic and cathodic polarization curves were obtained at a scan rate of 0.001 Vs<sup>-1</sup> in the potential range from -1.0 to 0 V relative to the corrosion potential (E<sub>corr</sub>). Electrochemical impedance spectroscopy and potentiodynamic polarization studies were performed using electrochemical analyzer Gamry DE190 instrument. Inhibition efficiency was calculated using equation 3

$$IE\% = \frac{R_{i_{ct}} - R_{o_{ct}}}{R_{i_{ct}}} \times 100 \quad \dots \dots \dots \quad 3$$

### E. SURFACE ANALYSIS

The surface morphology of the mild steel specimens immersed in 1 M HNO<sub>3</sub> without and with 10.0 g/L of

inhibitors was investigated using SEM analysis. Measurements were performed using Samsung 174IG machine, equipped with digital imaging and 27 mm photography system. SEM images were obtained by applying operating voltage of 15 – 30 kV.

### III. RESULTS FROM ANALYSIS

#### A. GRAVIMETRIC RESULTS

Experiments were performed with different concentrations of the inhibitors. From the weight loss data, the corrosion rates were determined from the slope of the plots of weight loss (mg/cm<sup>2</sup>) against time of exposure and the surface area (θ) and inhibition efficiency (IE%) determined using equations 4 and 5, respectively (Ikeuba et al., 2015; Ugi and Magu 2017; Singh et al., 2013)..

$$\theta = \frac{R_o - R_i}{R_o} \dots\dots\dots 4$$

$$IE\% = \left( \frac{R_o - R_i}{R_o} \right) \times 100 \dots\dots\dots 5$$

Where  $R_o$  and  $R_i$  are the corrosion rates in the absence and present of the various plant extracts. The values of the calculated corrosion rates of the metal, surface coverage and inhibition efficiencies of the inhibitors are shown in Table 1. It is observed that the corrosion rates of the metal decreases, surface coverage and inhibition efficiency of inhibitors increases with increase in extracts concentration which suggest a strong adhesion of the inhibition molecules on the metal surface (Dakeshwar and Fahmida, 2016; Fouda et al., 2017; Olusegun et al., 2016). The extracts showed maximum inhibition efficiency of 98.9 % 81.3 % and 69.7 % at an optimum concentration of 10.0 g/L for CAEAA, CEEAA and CSEAA, respectively

Conc. (g/L)	CEEAA			CAEAA			CSEAA		
	CR (mg/cm <sup>2</sup> /h)	θ	%IE	CR (mg/cm <sup>2</sup> /h)	θ	%IE	CR (mg/cm <sup>2</sup> /h)	θ	%IE
1 M HNO <sub>3</sub>	1.061	-	-	1.061	-	-	1.061	-	-
1.0 g/L	0.687	0.352	35.2	0.388	0.634	63.4	0.506	0.523	52.3
2.0 g/L	0.467	0.560	56.0	0.310	0.708	70.8	0.401	0.622	62.2
3.5 g/L	0.410	0.614	61.4	0.201	0.811	81.1	0.320	0.698	69.8
7.0 g/L	0.399	0.624	62.4	0.038	0.964	96.4	0.261	0.754	75.4
10.0 g/L	0.321	0.697	69.7	0.011	0.989	98.9	0.198	0.813	81.3

Table1: Calculated values of corrosion rates, surface coverage and inhibition efficiency for mild steel coupons in 1 M HNO<sub>3</sub> in the absence and presence of CAEAA, CEEAA and CSEAA at 30°C.

#### B. GASOMETRIC RESULTS

When the electrochemical corrosion reaction involve a cathodic process of hydrogen depolarization, the corrosion rate increases exponentially with rise in temperature, according to Arrhenius-type dependence (Al-Amiery et al., 2014; Patel et al., 2013; Gopal et al., 2015). Thus to evaluate the stability of adsorbed layer/film of inhibitor on mild steel surface as well as activation parameters of the corrosion process of steel in acidic media, hydrogen evolution

measurements were carried out at 30, 40, and 60°C in the absence and presence of extracts at various concentrations for 1 hour immersion time as shown in Figures 1 – 3. Results thus obtained are shown in Table 2. It is observed that inhibition efficiencies decrease with increasing temperature. This suggest increase rate in the dissolution process of mild steel coupons and desorption of the inhibitors from the metal surface with temperature (Ugi et al., 2015; Okewale and Olaitan 2017; Sharma et al., 2015; Kadhum et al., 2014).

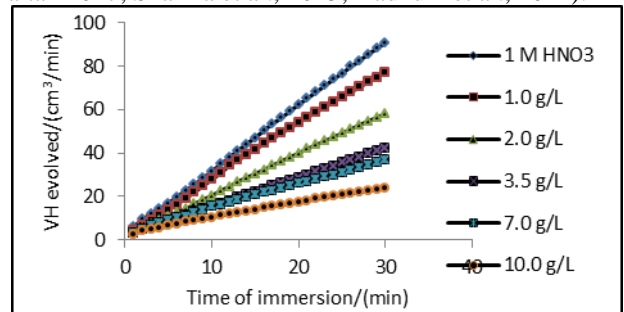


Figure 1: Variation of volume of hydrogen gas evolved with time for MS in 1 M HNO<sub>3</sub> in the presence of various concentrations of CAECAL at 303 K

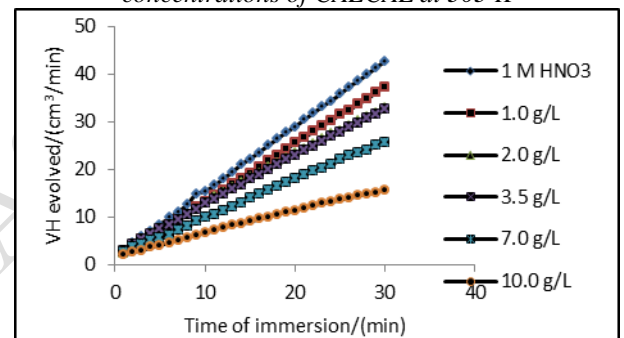


Figure 2: Variation of volume of hydrogen gas evolved with time for MS in 1 M HNO<sub>3</sub> in the presence of various concentrations of CEECAL at 303 K

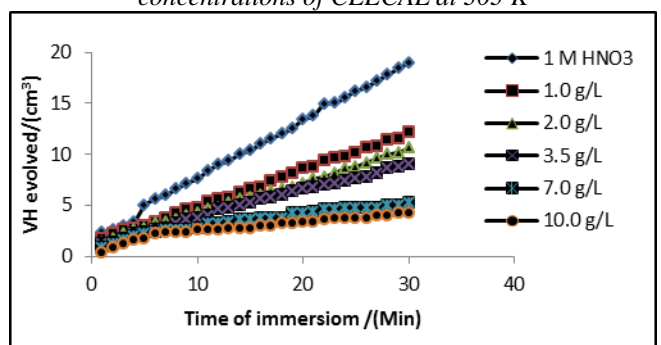


Figure 3: Variation of volume of hydrogen gas evolved with time for MS in 1 M HNO<sub>3</sub> in the presence of various concentrations of CSECAL at 303 K

	Conc. (g/L)	CR (mg/cm <sup>2</sup> /h)			θ			% IE		
		303K	313K	333K	303K	313K	333K	303K	313K	333K
CSEAA	1 M HNO <sub>3</sub>	10.558	17.366	23.097	-	-	-	-	-	-
	1.0 g/L	5.011	10.326	20.015	0.525	0.405	0.133	52.5	40.5	13.3
	2.0 g/L	5.012	8.773	14.910	0.525	0.495	0.354	52.5	49.5	35.4
	3.5 g/L	3.221	7.291	13.167	0.695	0.580	0.430	69.5	58.0	43.0
	7.0 g/L	2.521	4.333	7.472	0.761	0.750	0.676	76.1	75.0	67.6
	10.0 g/L	2.135	3.999	6.761	0.798	0.770	0.707	79.8	77.0	70.7
CAEAA	1 M HNO <sub>3</sub>	10.558	17.366	23.097	-	-	-	-	-	-
	1.0 g/L	5.000	8.090	15.744	0.526	0.534	0.318	52.6	53.4	31.8

	2.0	4.177	6.997	11.796	0.604	0.597	0.489	60.4	59.7	48.9
	g/L									
	3.5	2.547	4.713	9.793	0.759	0.729	0.576	75.9	72.9	57.6
	g/L									
	7.0	1.894	3.278	6.195	0.821	0.811	0.732	82.1	81.1	73.2
	g/L									
	10.0	0.113	1.542	3.847	0.989	0.911	0.833	98.9	91.1	83.3
	g/L									
CEEAA	1 M	10.558	17.366	23.097	-	-	-	-	-	-
	HNO <sub>3</sub>									
	1.0	4.287	8.274	16.977	0.594	0.524	0.265	59.4	52.4	26.5
	g/L									
	2.0	3.227	7.109	13.634	0.694	0.591	0.410	69.4	59.1	41.0
	g/L									
	3.5	2.915	5.761	10.744	0.724	0.668	0.535	72.4	66.8	53.5
	g/L									
	7.0	2.108	3.101	6.382	0.800	0.821	0.724	80.0	82.1	72.4
	g/L									
	10.0	1.038	2.558	4.517	0.902	0.853	0.804	90.2	85.3	80.4
	g/L									

Table 2: Calculated values of corrosion rates, surface coverage and inhibition efficiency for mild steel coupons in 1 M HNO<sub>3</sub> in the absence and presence of CAEAA, CEEAA and CSEAA at 30°C

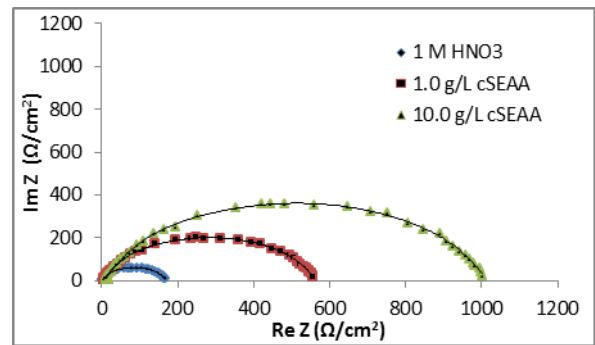


Figure 6: Nyquist plots for MS in 1 M HNO<sub>3</sub> in the presence of various concentrations of CSEAL

The obtained values for the charge transfer resistance and parallel film capacitance are listed in Table 3. As seen from Table 3, the value of  $R_{ct}$  increases with increase in the concentrations of the inhibitor. The capacitance of parallel film ( $C_{dl}$ ) was calculated from equation 6.

$$C_{dl} = \frac{1}{R_{ct} 2\pi f_{max}} \quad \dots\dots\dots 6$$

Where  $R_{ct}$  is the charge transfer resistance and the  $f_{max}$  is the frequency of the maximum curve. Table 3 shows that  $C_{dl}$  values decreased when the concentration of the inhibitor molecules increased. The decrease in  $C_{dl}$  might arise from a decrease in local dielectric constant and/or an increase of the electrical double layer thickness which might arise from substitution of preadsorbed water molecules on the metal/electrolyte interface by adsorbed organic constituents of the extracts whose dielectric constant is lower, suggesting that inhibitor molecules function by adsorption at the metal/solution interface (Shi et al., 2016; Sudershan et al., 2016; Ghulamullah et al., 2015).

Conc. (g/L)	CAEAAAL			CEEAAAL			CSEAAAL		
	$R_{ct}$ (Ωcm <sup>2</sup> )	$C_{dl}$ (μFcm <sup>-2</sup> )	% IE	$R_{ct}$ (Ωcm <sup>2</sup> )	$C_{dl}$ (μFcm <sup>-2</sup> )	% IE	$R_{ct}$ (Ωcm <sup>2</sup> )	$C_{dl}$ (μFcm <sup>-2</sup> )	% IE
1 M HNO <sub>3</sub>	187	9.44 x 10 <sup>-5</sup>	-	187	9.44 x 10 <sup>-5</sup>	-	187	9.44 x 10 <sup>-5</sup>	-
1.0 g/L	1,305	1.02 x 10 <sup>-5</sup>	85.67	1,192	2.23 x 10 <sup>-5</sup>	84.31	582	3.73 x 10 <sup>-5</sup>	67.87
10.0 g/L	2,609	5.4 x 10 <sup>-6</sup>	92.81	1,502	1.18 x 10 <sup>-5</sup>	87.53	1,007	1.76 x 10 <sup>-5</sup>	81.31

Table 3: EIS parameters for MS without and with different concentrations of CAEAA, CEEAA and CSEAA in 1 M HNO<sub>3</sub>

D. POTENTIODYNAMIC POLARIZATION MEASUREMENTS

The anodic and cathodic polarization curves of mild steel electrode in 1 M HNO<sub>3</sub> medium with and without the various concentrations of CAEAA, CEEAA and CSEAA are presented in Figures 7 - 9. This type of plots have been produced earlier by Mourya et al., (2014); Okewale and Olaitan (2017). The electrochemical parameters such as corrosion potential ( $E_{corr}$ ) and corrosion current density ( $I_{corr}$ ) were obtained from the intersection of anodic and cathodic Tafel slopes of the polarization curves and this values are shown in Table 4. It is obvious from table 4 that both the cathodic and anodic curves showed lower current densities in the presence of the extract than those recorded in the free solution (1 M HNO<sub>3</sub>). This is suggesting that both extracts reduce the rate of anodic MS dissolution in the acid as well as the cathodic hydrogen ion reduction. This effect can be

C. ELECTROCHEMICAL IMPEDANCE SPECTROSCOPY MEASUREMENTS

Typical Nyquist plots obtained for MS in 1 M HNO<sub>3</sub> without and with various concentrations of the studied inhibitors are shown in Figures 4 - 6. The Nyquist plots show depressed semicircles due to non-ideal behaviour of the electrochemical interface of the MS in the aggressive electrolyte. Nyquist plot of one capacitive loop exhibiting an extended semicircle in the complex impedance plane both in uninhibited and inhibited solutions, an indication that corrosion rate is controlled by charge transfer resistance (Ugi et al., 2016a; Gadaw and Motawea 2017; Sudershan et al., 2016). The impedance diagrams obtained increases in diameter as inhibitor concentration increases indicating that the presence of inhibitor molecules strengthens the inhibitive film occurring through defects of this film with increase in *Ageratina altissima* extracts concentration.

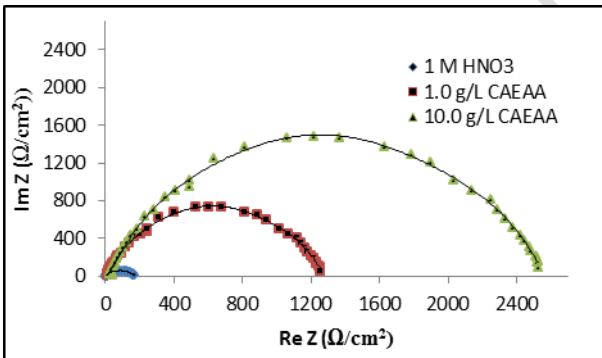


Figure 4: Nyquist plots for MS in 1 M HNO<sub>3</sub> in the presence of various concentrations of CAEAL

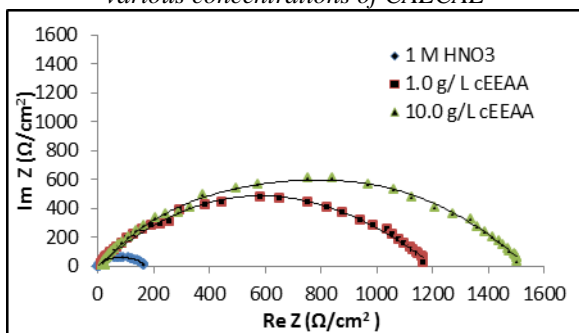


Figure 5: Nyquist plots for MS in 1 M HNO<sub>3</sub> in the presence of various concentrations of CEECAL

attributed to the blockage of active sites on the MS surface by the adsorbed film of the molecules of the studied inhibitors as earlier reported by Sudershan et al, (2016); Ugi et al., (2015); Al-Otaibi et al., (2014). From the results obtained, the changes of  $E_{corr}$  are less than 85mV for the studied plant extracts, this suggest that both inhibitors act as mixed type for the corrosion of mild steel in 1 M  $HNO_3$  medium. The polarization curves in the presence of both inhibitors show similar cathodic features as the 1 M  $HNO_3$  suggesting that the inhibitors do not change the mechanism of the cathodic hydrogen gas evolution associated with the corrosion process (ugi et al., 2015; Louis et al., 2017; Gadow and Motawea 2017). Similar observations were notices with the anodic part of the polarization curves.

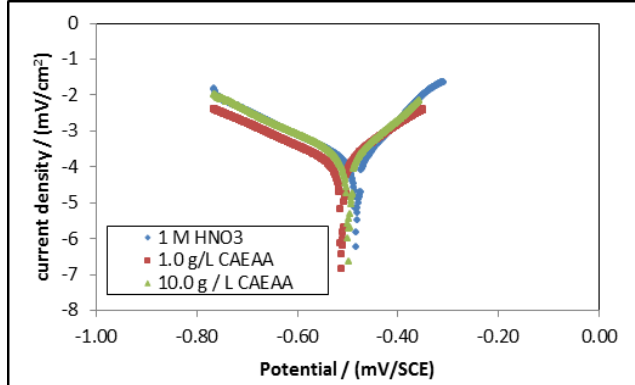


Figure 7: Tafel plots showing effect of increasing concentrations of CAEAA on corrosion of MS in 1 M  $HNO_3$  solutions

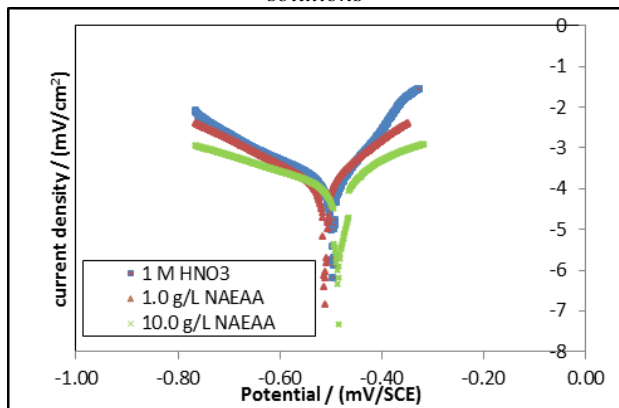


Figure: 8: Tafel plots showing effect of increasing concentrations of CEEAA on corrosion of MS in 1 M  $HNO_3$  solutions

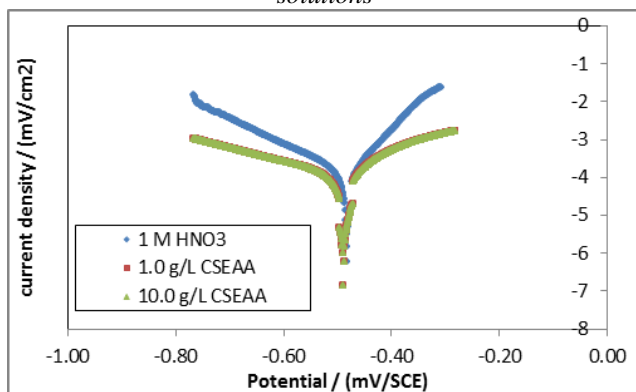


Figure 9: Tafel plots showing effect of increasing concentrations of CSEAA on corrosion of MS in 1 M  $HNO_3$  solutions

	Conc. (g/L)	$I_{corr}$ ( $mA/cm^2$ )	$E_{corr}$ (mV)	$B_c$ (mV/dec)	$\beta_a$ (mV/dec)	$\theta$	$IE_i$ (%)
CEEAA	1 M $HNO_3$	21.87	-917	228	156	-	-
	1.0 g/L	8.903	-772	217	111	0.593	59.3
	10.0 g/L	4.191	-229	128	90	0.808	80.8
CAEAA	1 M $HNO_3$	21.87	-917	228	156	-	-
	1.0 g/L	2.091	-553	141	101	0.904	90.4
	10.0 g/L	1.172	-211	94	65	0.946	94.6
CSEAA	1 M $HNO_3$	21.87	-917	228	156	-	-
	1.0 g/L	11.954	-444	128	98	0.453	45.3
	10.0 g/L	5.003	-219	88	52	0.771	77.1

Table 4: Potentiodynamic polarization parameters for MS without and with different concentrations of CAEAA, CEEAA and CSEAA in 1 M  $HNO_3$

### E. SEM ANALYSIS

Scanning electron microscope images of polished surface of mild steel coupons retrieved from MS in 1 M  $HNO_3$  in the absence and presence of 10 g/L of CAEAA, CEEAA and CSEAA are shown in Figures 10 (a) – (d). The surface of the mild steel coupon retrieved from the blank 1 M  $HNO_3$  solution encountered noticeable damage and marked with series of deep pits due to uninhibited acid corrosion. The mild steel retrieved from the inhibitor-containing aggressive solution present relatively smooth surface, which can be explained from the protection of the coupon surface by the adsorbed film of inhibitor molecules according to the work of Sudershan et al, (2016); Dakeshwar and Fahmida, (2016); Olusegun et al., (2016)

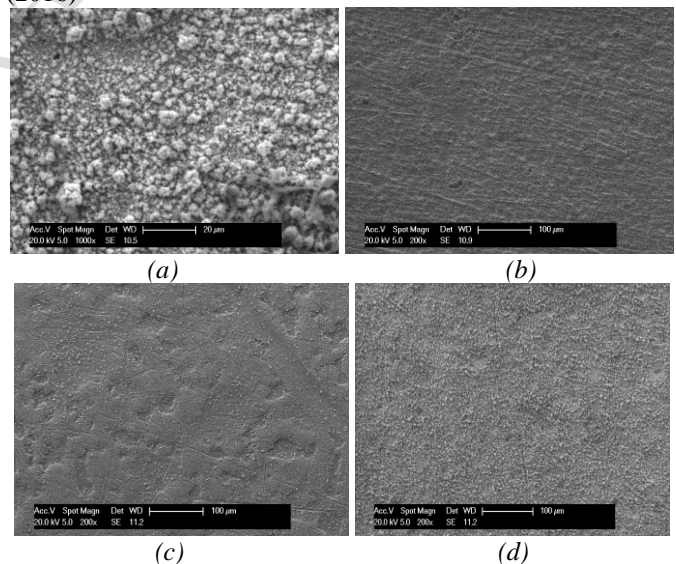


Figure 10: Scanning Electron Microscopic images of (a) MS in 1 M  $HNO_3$ , (b) MS in 1 M  $HNO_3$  + 10 g/L CAEAA, (c) MS in 1 M  $HNO_3$  + 10 g/L CEEAA, and (d) MS in 1 M  $HNO_3$  + 10 g/L CSEAA

### F. THERMODYNAMIC PARAMETERS

Figure 11 - 13 shows Arrhenius plots for the mild steel in 1 M  $HNO_3$  solutions in the absence and presence of the extracts. The activation energies ( $E_a$ ) were expressed by the Arrhenius equation 7:

$$\ln R_c = \ln A - \frac{E_o}{RT} \quad \dots\dots\dots 7$$

Where  $R_c$  is the corrosion rate,  $E_a$  is the apparent effective activation energy,  $R$  is the general gas constant, and  $A$  is the Arrhenius pre-exponential factor. The values of calculated activation energies are shown in Table 5.

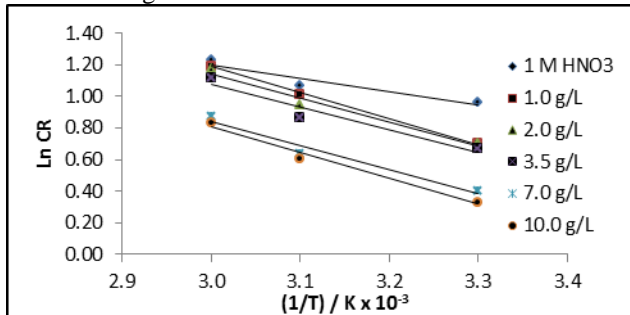


Figure 11: Arrhenius plots for mild steel in 1 M HNO<sub>3</sub> solutions in the absence and presence of CAEAA

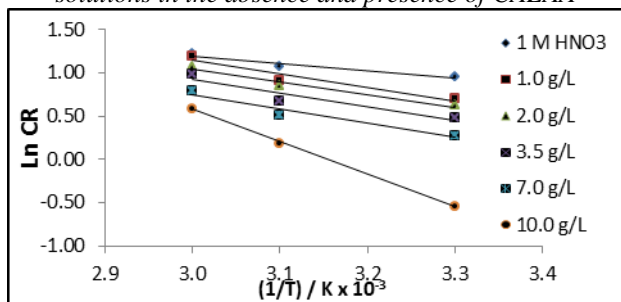


Figure 12: Arrhenius plots for mild steel in 1 M HNO<sub>3</sub> solutions in the absence and presence of CEEAA

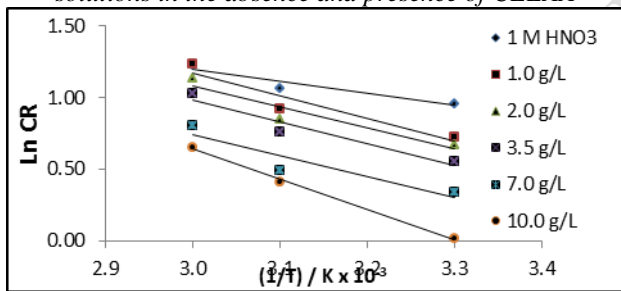


Figure 13: Arrhenius plots for mild steel in 1 M HNO<sub>3</sub> solutions in the absence and presence of CSEAA

The data in Table 5 show that the activation energies ( $E_a$ ) of the corrosion of mild steel in 1 M HNO<sub>3</sub> in the presence of the extracts are higher than that in the free acid solution, suggesting that a physical adsorption occurs in the first stage (Ugi et al., 2016b; Ikeuba et al., 2015; Atta et al., 2014). Increase in activation energies suggested an appreciable decrease in the adsorption of the inhibitor on the mild steel surface with increase in temperature. The enthalpy of activation ( $\Delta H^*$ ) and the entropy of activation ( $\Delta S^*$ ) for the corrosion of mild steel in 1 M HNO<sub>3</sub> was estimated using the transition state equation 8.

$$R_c = \frac{KT}{h} \exp\left(\frac{\Delta S^*_i}{R}\right) \exp\left(\frac{-\Delta H^*_i}{RT}\right) \quad \dots\dots\dots 8$$

where  $K$  is the Boltzmann constant,  $h$  is the Planck constant,  $A$  is Arrhenius pre-exponential factor,  $T$  is the absolute temperature and  $R_c$  is corrosion rate. The plots and values of  $\Delta H^*$  and  $\Delta S^*$  obtained are given in Figures 14 – 16 and Table 5 respectively. Inspection of Table 5 show higher

values for  $\Delta H^*$  in the presence of the inhibitors, suggesting a higher protection efficiency observed for the system (Peter et al., 2015; Patel et al., 2013). The  $\Delta S^*$  values in the absence and presence of the inhibitors are negative, indicating the activation stage of the adsorption process is controlled by associative interactions between the iron and the inhibitor molecules rather than dissociative formation of iron and water molecules (Sudershan et al., 2016; Fouda et al., 2017).

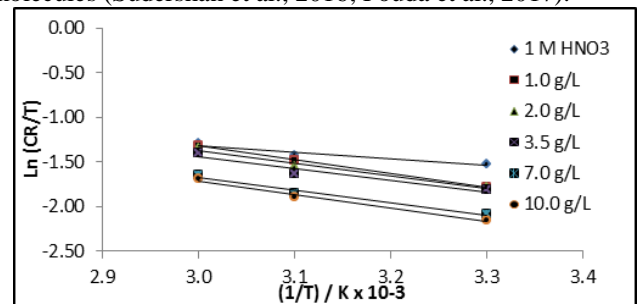


Figure 14: Eyring transition state plots for mild steel in 1 M HNO<sub>3</sub> in the absence and presence of CAEAA

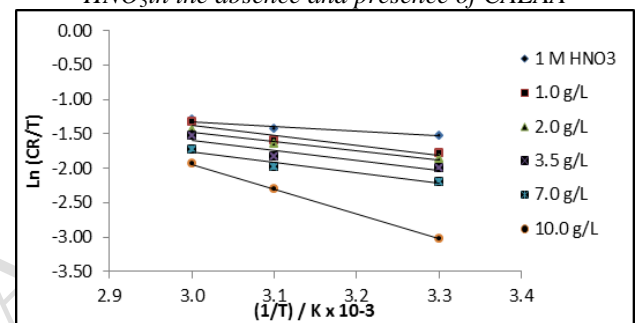


Figure 15: Eyring transition state plots for mild steel in 1 M HNO<sub>3</sub> in the absence and presence of CEEAA

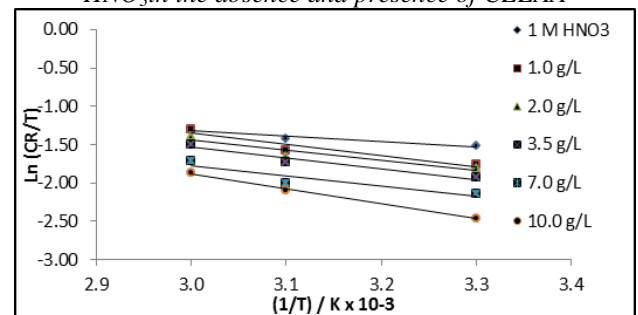


Figure 16: Eyring transition state plots for mild steel in 1 M HNO<sub>3</sub> in the absence and presence of CSEAA

Conc. (g/L)	CEEAA			CAEAA			CSEAA		
	E <sub>a</sub>	ΔH <sub>abs</sub>	ΔS <sub>abs</sub>	E <sub>a</sub>	ΔH <sub>abs</sub>	ΔS <sub>abs</sub>	E <sub>a</sub>	ΔH <sub>abs</sub>	ΔS <sub>abs</sub>
1 M HNO <sub>3</sub>	7.1	-10.1	-77.3	7.1	-10.1	-77.3	7.1	-10.1	-77.3
1.0 g/L	12.9	-17.6	-155.9	11.7	-12.5	-151.2	15.6	-15.8	-151.2
2.0 g/L	13.5	-21.8	-162.0	13.9	-15.9	-169.8	15.9	-15.9	-155.4
3.5 g/L	15.7	-23.0	-167.3	14.0	-17.7	-171.8	18.5	-16.8	-161.3
7.0 g/L	16.9	-23.7	-170.8	15.8	-19.9	-188.0	20.1	-17.4	-168.2
10.0 g/L	20.0	-26.9	-199.7	18.5	-21.2	-197.4	22.6	-21.8	-188.9

Table 5: Activation parameters for mild steel in 1 M HNO<sub>3</sub> in the absence and presence of the plant extracts

### G. ADSORPTION CONSIDERATION

The most probably mechanism by which organic compounds inhibit metal corrosion is the adsorption of organic

molecules on the metal surface (Sudershan et al, 2016; Ugi et al., 2015; Gadow and Motawea 2017). Adsorption isotherm is one technique where basic information on the interaction between the inhibitor and the mild steel surface can be obtained. In the present study, several adsorption isotherms were tested in an attempt to fit the experimental data but only the Langmuir adsorption isotherm provided acceptable linear fits based on the near unity values of the correlation coefficient values (Figures 17 – 19). The Langmuir isotherm may be formulated as equation 9:

$$\frac{c}{\theta} = \frac{1}{k} + c \quad \dots\dots\dots 9$$

Where  $c$  is the concentration of inhibitor and  $k$  equals the equilibrium constant for the adsorption/desorption process. The values of  $K_{ads}$  obtained at different temperatures from the intercept of the isotherm plots are given in Table 6. The significant large values of  $K_{ads}$  obtained for the studied inhibitors suggest strong adsorption of the inhibitor molecules on the mild steel surface (Sudershan et al, 2016; Ugi et al., 2015; Gadow and Motawea 2017). The standard adsorption free energy  $\Delta G_{ads}$  values (shown in Table 6) were obtained using the equation 10:

$$k = \frac{1}{55.5} \exp \frac{-\Delta G_{ads}}{RT}$$

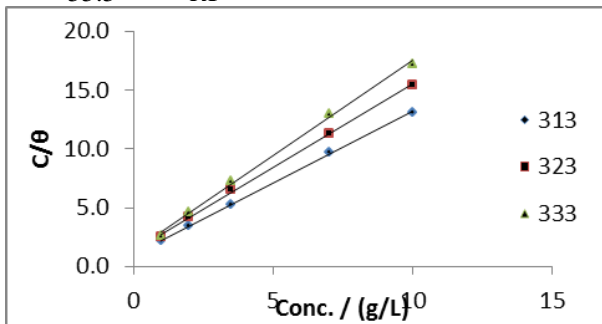


Figure 17: Langmuir adsorption isotherm for mild steel in 1 M HNO<sub>3</sub> in the absence and presence of CAEAA

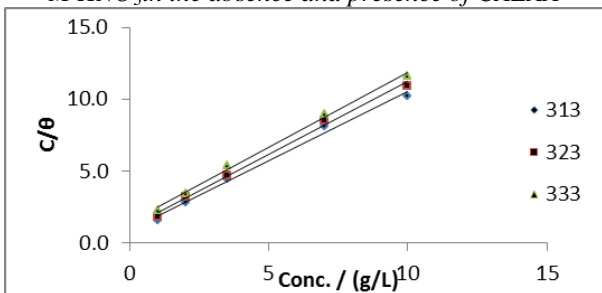


Figure 18: Langmuir adsorption isotherm for mild steel in 1 M HNO<sub>3</sub> in the absence and presence of CEEAA

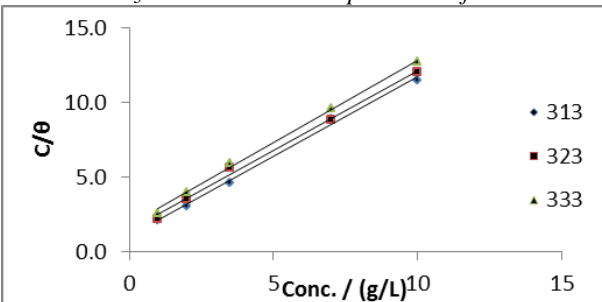


Figure 19: Langmuir adsorption isotherm for mild steel in 1 M HNO<sub>3</sub> in the absence and presence of CSEAA

Where  $R$  is the gas constant,  $T$  is the temperature, and  $55.5$  is the molar concentration of water in aqueous solution. Negative values of  $\Delta G_{ads}$  indicate spontaneity and stability of the adsorption layer. The values of the free energy obtained which were below  $-40\text{kJ/mol}$  also suggests a physical adsorption mechanism for adsorption of the inhibitor on the mild steel surface in 1 M HNO<sub>3</sub> solution (Ikeuba et al., 2015).

Temp. (K)	CAEAA				CEEAA				CSEAA			
	k (g/L)	R <sup>2</sup>	Slope	$\Delta G_{ads}$ (kJ/mol)	k (g/L)	R <sup>2</sup>	Slope	$\Delta G_{ads}$ (kJ/mol)	k (g/L)	R <sup>2</sup>	Slope	$\Delta G_{ads}$ (kJ/mol)
313	1.0131	0.999	1.2147	-10.485	0.8772	0.991	0.9671	-10.111	0.625	0.996	1.038	-9.029
323	1.3015	0.999	1.4263	-11.493	1.075	0.994	1.012	-10.769	0.860	0.980	1.038	-10.156
333	1.3467	0.997	1.6157	-11.943	1.476	0.996	1.037	-12.197	1.070	0.978	1.069	-11.062

Table 6: Adsorption parameters for mild steel in 1 M HNO<sub>3</sub> containing CAEAA, CEEAA and CSEAA

#### IV. CONCLUSION

- ✓ CAEAA, CEEAA and CSEAA showed appreciable corrosion inhibition performance for mild steel in 1 M HNO<sub>3</sub>.
- ✓ The adsorption behavior of CAEAA, CEEAA and CSEAA on mild steel in 1 M HNO<sub>3</sub> obeys the Langmuir adsorption isotherm and involves a physical adsorption mechanism.
- ✓ Inhibition efficiency of the studied inhibitors increases with increasing concentration and decreases with increase in temperature.
- ✓ SEM micrographs proved that the mild steel surface immersed in the 1 M HNO<sub>3</sub> in the presence of CAEAA, CEEAA and CSEAA is protected from direct acid attack.
- ✓ Results obtained from electrochemical methods are in good agreement with those of gravimetric measurements.

#### REFERENCES

- [1] Al-Amiery A. A., Abdul A., Kadhum H. Kadhum A, Mohamad A. B., How C. K. and Junaedi S. (2014) Inhibition of Mild Steel Corrosion in Sulfuric Acid Solution by New Schiff Base. *Materials*, 7: 787-804
- [2] Al-Otaibi M. S., Al-Mayouf A. M., Khan M., Mousa A. A., Al-Mazroa S. A., and Alkhatlan H. (2014) corrosion inhibitory action of some plant extracts on the corrosion of mild steel in acidic media. *Science Direct*. 7(3): 340 – 346
- [3] Atta A. M., El-Mahdy G. A, Al-Lohedan H. A and Al-Hussain S. A (2014) Inhibition of Mild Steel in Acidic Medium by Magnetite Myrrh Nanocomposite. *International Journal of Electrochemical Science*. 9: 8446 – 8457
- [4] Dakeshwar, K. V. and Fahmida, K. (2016) Green approach to corrosion inhibition of mild steel in hydrochloric acid medium using extracts of spirogyra algae. *Green chemistry letters and reviews*, 9 (1): 52 – 60.
- [5] Fouda, A. S., El-Ewady G. and Ali H. (2017) Modazar as promising corrosion inhibitor of carbon steel in hydrochloric acid solution, *Green Chemistry Letters and Reviews*. 10(2): 88 – 100

- [6] Gadow H. S. and Motawea M. M. (2017) Investigation of the corrosion inhibition of carbon steel in hydrochloric acid solution by using ginger root extracts. *Royal society of chemistry*. 7: 24576 - 24588
- [7] Ghulamullah K., Kazi M, Newaz N., Wan J., Basiru H., Binti M. A., Fadhil L. F. and Ghulam M. K. (2015) Application of Natural Product Extracts as Green Corrosion Inhibitors for Metals and Alloys in Acid Pickling Processes - A review. *International Journal of Electrochemical Science*. 10 (2015): 6120 – 6134
- [8] [8] Gopal, J., Shadma, A., Shanthi S. and Rajiv P. (2015) Musa paradisica peel extract as green corrosion inhibitor for mild steel in HCl solution, *ScienceDirect*. 90: 107 – 117
- [9] Ikeuba, A. I., Ita, B. I., Etiuma R.A., Bassey V.M., Ugi B. U. and Kporokpo E. B. (2015) Green corrosion inhibitors for mild steel in H<sub>2</sub>SO<sub>4</sub> solution: Comparative study of flavonoids extracted from *Gongronemalatifolium* with crude extract. *Journal of Chemical and Process Engineering*, 34: 1 – 9
- [10] Kadhum AH, Mohamad AB, Hammed LA, Al-Amiery AA, San NH, Musa YA. (2014) Inhibition of mild steel corrosion in hydrochloric acid solution by new coumarin. *Materials*. 7: 4335-4348.
- [11] Louis H., Japari J., Sadia A., Philip M. and Bamanga A. (2017) Photochemical screening and corrosion inhibition of *Poupartiarbirrea* back extract as a potential green inhibitor for mild steel in 0.5 M H<sub>2</sub>SO<sub>4</sub> solution, *World news of natural sciences*. 10(2017): 95 – 100
- [12] Mourya P., Sitashree B. and Singh M. M. (2014) corrosion inhibition of mild steel in acidic solution by *Tagetes erecta* (Marigold flower) extract as green inhibitor. *Corrosion Science*, 85(2014): 352 – 363
- [13] Okewale A. O and Olaitan A. (2017) The use of rubber leaf extract as a corrosion inhibitor for mild steel in acidic solution, *International journal of material and chemistry*. 7(1): 5 – 13
- [14] Olesegun S. J., Okoronkwo E. A., Okotete A. E., and Ajayi O. A. (2016) Gravimetric and electrochemical studies of corrosion inhibition potential of acid and ethanol extract of siam weed on mild steel, *Leonardo Journal of Sciences*. 9(2): 25 – 42
- [15] Patel N. S., Jauhariand S., Mehta G. N., Ad-Deyab S. S., Warad I. and Hammouti B. (2013) Mild Steel Corrosion by Various Plant Extracts in 0.5 M Sulphuric acid". *Int. J. of Electrochem. Sci*. 8(2013): 2635 – 2655.
- [16] Peter A., Obot I. B. and Sharma S. K. (2015) Use of natural gums as green corrosion inhibitors: an overview. *International Journal of Industrial Chemistry*. 6(3): 153-164
- [17] Sharma K. S, Anjali Peter & Obot I. B. (2015) Potential of *Azadirachtaindica* as a green corrosion inhibitor against mild steel, aluminium and tin: a review. *Journal of analytical science and technology*. 6 : 26 – 41
- [18] Shi M., Hong-Qun L. and Nian-Bing L. (2016) Plant extract as green corrosion inhibitors for steel in sulphuric acid. *Chemical papers*, 70(9): 1131 – 1143
- [19] Singh, A., Singh V. K., and Quraishi, M. A. (2013) Inhibition of mild steel corrosion in HCl solution using *Pipali* (*piper longum*) fruit extract. *Arabian journal of science and Engineering*, 38 (1): 85 – 97
- [20] Sudershan K., Hemlata V. And Ebenso E. E. (2016) Experimental and theoretical studies on inhibition of mild steel corrosion by some synthesized polyurethane tri-block co-polymers, *Scientific report*, 6 article number: 30937, doi: 10.1038/srep30937
- [21] Ugi B. U, Uwah I. E, Okafor P. C, Ekerete Jackson, Ejim S. E and Nya N. E. (2016) Sulphuric Acid Corrosion of Mild Steel in the Stem Extracts of *Cnidocolusaconitifolius* Plant *Journal of Applied Chemical Science International* 5(4): 209 – 216
- [22] Ugi B. U., Ekerete Jackson, Ikeuba A. I. and Uwah I. E. (2015) *Mangifera indica* Leave Extracts as Organic Inhibitors on the Corrosion of Zinc Sheet in 5 M H<sub>2</sub>SO<sub>4</sub> Solution. *Journal of Applied Sciences & Environmental Management* 19(1): 145 – 152
- [23] Ugi, B. U. and Magu, T. O. (2017) Inhibition, Adsorption and Thermodynamic Investigation of Iron Corrosion by Green Inhibitors in Acidic Medium. *The International Journal Of Science & Technoledge* 5(4): 56 – 64
- [24] Ugi, B. U., Obeten, M. E., Uwah I. E. and Okafor P. C. (2016) Aluminium corrosion abatement using non toxic and eco-friendly organic inhibitors. *Journal of Global Ecology and Environment* 4(4): 242 – 252